



Original Article

Drilling optimisation for additively manufactured PC/ABS parts: Effects of shell layer count in the MEX process

Fırat MAVI¹, Kemal AYAN², Nail ASLAN², Sırrı Can POLAT²,
İbrahim Etem SAKLAKOĞLU¹, Nurşen SAKLAKOĞLU²

¹Department of Mechanical Engineering, Ege University Faculty of Engineering, İzmir, Türkiye

²Department of Mechanical Engineering, Manisa Celal Bayar University, Faculty of Engineering and Natural Sciences, Manisa, Türkiye

ARTICLE INFO

Article history

Received: 02 March 2025

Revised: 11 May 2025

Accepted: 21 May 2025

Key words:

Additive manufacturing, drilling, material extrusion (MEX), optimization, shell layer count.

ABSTRACT

Although additive manufacturing enables the production of near-net-shape geometries, dimensional accuracy can vary due to both design and process-related factors. Features that exceed the critical overhang angle may suffer unavoidable distortions, even with support structures. To ensure dimensional precision—particularly in critical hole features—it is often preferable to fabricate the main structure without holes and subsequently perform drilling as a secondary machining operation. Moreover, additively manufactured parts are increasingly used as core layers in sandwich structures assembled with rivets, further highlighting the importance of post-process drilling. This study investigates the effect of shell layer count on the drilling performance of PC/ABS parts fabricated using the Material Extrusion (MEX) method. Samples with three different shell layer counts and 50% infill were produced, and drilling operations were carried out at varying feed rates and spindle speeds. Surface roughness of the printed plates was measured using a profilometer, while hole diameters and cylindricity were assessed via a coordinate measuring machine (CMM). Delamination was evaluated through stereomicroscope imaging. The results indicate that shell layer count does not have a significant effect on surface roughness for the top and lateral surfaces—except for Rz on the lateral surface, where a statistically significant difference was observed. Hole diameter deviation increases with feed rate and decreases with spindle speed, with no significant correlation to shell count. Cylindricity deteriorates at higher feed rates, while spindle speed and shell count show no consistent effects. Delamination remained low for 4 and 8 shell layers but increased notably at 12. Based on the findings, employing 4 or 8 shell layers and performing drilling at a feed rate of 50 mm/min and spindle speed of 1200 rpm is recommended for optimal results.

Cite this article as: Mavi, F., Ayan, K., Aslan, N., Polat, S. C., Saklakoğlu, İ. E., & Saklakoğlu, N. (2025). Drilling optimisation for additively manufactured PC/ABS parts: Effects of shell layer count in the MEX process. *J Adv Manuf Eng*, 6(1), 22–32.

*Corresponding author.

*E-mail address: firat.mavi@ege.edu.tr



INTRODUCTION

Material Extrusion (MEX), also referred to as Fused Filament Fabrication (FFF) or Fused Deposition Modeling (FDM), is an additive manufacturing technique in which thermoplastic materials are deposited layer by layer through a heated nozzle, following the geometry defined by a digital 3D model [1]. The process supports a wide range of thermoplastics in filament or pellet form [2] and enables the fabrication of complex geometries without the need for molds or specialized tooling. This makes MEX particularly suitable for low-volume production, rapid prototyping, and design iterations. However, it still faces certain limitations—such as relatively high unit costs compared to traditional mass-production methods.

However, the production of certain geometries—particularly those involving overhangs that exceed the critical build angle—requires the use of support structures. Although these structures are typically easy to remove post-process, they contribute to increased material consumption and roughen the part's surface, which in turn raises overall production costs. On the other hand, waste materials are generated, which either contribute to environmental pollution or necessitate additional costs for their disposal. A practical strategy to mitigate these issues involves subdividing complex geometries into multiple subassemblies that can be printed independently and later joined. In such cases, mechanical fasteners—such as bolts, nuts, or rivets—are often preferred for assembly due to their ease of disassembly and reusability. This approach, however, necessitates post-process drilling of the printed parts to accommodate the fasteners [3].

Although it is possible to incorporate holes directly into part designs and fabricate them using the MEX process, there are often cases where printed components must be modified post-production to meet specific or evolving requirements. In cases where manufacturing must accommodate several different requirements, parts can be initially printed as solid base models without holes, and the necessary holes can be drilled later at the required positions. This approach introduces flexibility into the production process. Since base products capable of meeting varying hole placement demands depending on the order type can be prepared in advance, it may also help reduce order delivery times. Drilling is also more practical and cost-effective than discarding or reprinting large components due to hole placement errors. However, the final hole quality is influenced by the material properties, process parameters, and hole orientation within the design. Holes printed at steep angles (above a critical threshold) typically require support structures for stability. Despite this, such holes often suffer from poor dimensional accuracy and geometric irregularities due to instability and support removal issues. Furthermore, post-processing steps—such as support removal or surface finishing—can further distort the hole geometry, making it unsuitable for precision applications [4]. Therefore, drilling is often a more reliable method for producing accurate and well-tolerated holes in MEX-fabricated parts.

Moreover, during the printing process, creating holes directly with a 3D printer requires the print nozzle to pause or change direction, which further increases the already lengthy printing time. In contrast, drilling holes as a secondary operation takes significantly less time compared to printing them during the manufacturing process. Kartal and Kaptan [5], demonstrated this by comparing different cutting tools for post-processing PLA parts fabricated with 100% infill, ultimately identifying those that maintained hole quality and minimized surface defects during drilling.

Among the various thermoplastics used in MEX, Acrylonitrile Butadiene Styrene (ABS) is well known for its toughness and favorable mechanical properties. However, it also presents challenges such as warping, poor dimensional stability, and poor adhesion to the build surface during cooling [6]. To overcome these limitations, ABS is frequently blended with other polymers to improve its printability and performance. One of the most effective blending materials is polycarbonate (PC), a high-strength, high-temperature-resistant thermoplastic that offers excellent durability, thermal resistance, and impact performance. Although PC is difficult to process on its own due to its high melt viscosity and brittleness under certain stress conditions, it complements ABS both mechanically and economically [7].

Blending PC with ABS results in a material that combines the strength and thermal stability of PC with the ductility and ease of processing of ABS, making PC/ABS blends particularly well-suited for MEX applications [8–10]. These blends are widely used in demanding sectors such as the automotive and aerospace industries, where parts are often subjected to mechanical loads and thermal fluctuations. Research into PC/ABS blends has highlighted their localized and anisotropic thermal deformation behaviors, which are especially relevant for post-processing and machining operations [11–14]. Recent advancements in understanding its thermal and plastic deformation properties indicate that PC/ABS blends perform significantly better in post-processing and machining operations compared to pure ABS. Because polycarbonate and ABS complement each other both technically and economically, PC/ABS blends have gained considerable attention for engineering applications that demand high toughness—particularly in the automotive industry [15].

In this study, the effect of the number of shell layers on the drilling performance of PC/ABS parts manufactured using the MEX method was investigated. Additionally, the study aimed to optimize drilling parameters by varying spindle speed and feed rate. Based on the authors' literature review, although limited research has explored the drilling of polycarbonate materials [16–18], no studies were found that specifically examine the drilling characteristics of PC/ABS blends. It is well established that shell layer count—referring to the number of outer perimeter walls—significantly influences the mechanical properties of MEX-manufactured parts. Increasing the shell count enhances the solid wall thickness around a hole, thereby improving tensile and bending strength [19]. Thicker shell walls can better withstand machining forces during drilling, while

parts with fewer shells may have insufficient structural support, leading to hole deformation or delamination. By experimentally linking shell count to drilling outcomes, this study aims to provide practical guidance on optimizing 3D printing parameters to ensure reliable post-machining performance. Understanding this relationship is essential for ensuring that additively manufactured parts can be safely and accurately drilled for fasteners or other functional features without compromising part integrity. Moreover, the MEX method enables the preservation of surface integrity by applying distinct infill patterns (e.g., grid, octet, etc.) within the internal regions of parts [20]. This feature allows MEX-produced components to function as meta-sandwich structures [21] or as core elements in sandwich material assemblies [22, 23]. When such structures are assembled using bolts, nuts, or rivets, post-process drilling may be necessary in the core sections [24]. Therefore, the primary objective of this study is to provide experimental data that support the optimization of drilling parameters for PC/ABS parts with varying shell layer counts, thereby contributing valuable insight to the current body of knowledge on additive manufacturing and secondary machining processes.

MATERIALS AND METHODS

Design and MEX Manufacturing

A rectangular prism-shaped sample with dimensions of 150 mm × 150 mm × 10 mm was designed for fabrication using the MEX method. To facilitate secure mounting on a vertical machining center (VMC), through-holes with a diameter of 8.2 mm were incorporated at all four corners as well as the center of the design (Fig. 1). A plate thickness of 10 mm was selected to balance the structural integrity required for stable drilling with the goal of minimizing material consumption. This thickness provides adequate rigidity to support consistent tool engagement and efficient chip

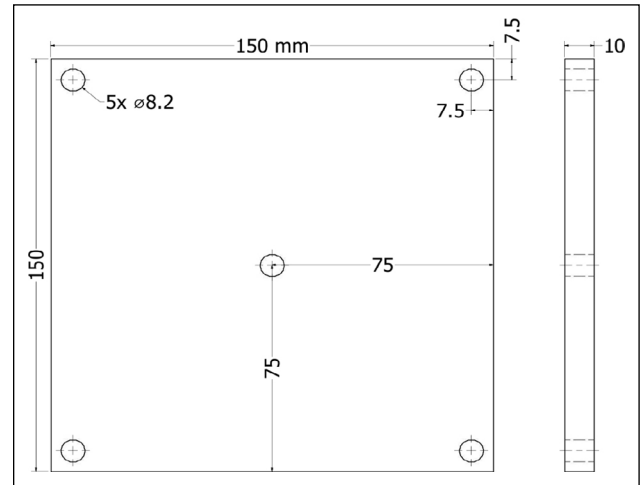


Figure 1. Technical drawings of sample plate.

evacuation, ensuring uniform machining conditions without compromising the part's mechanical stability.

Although minor delamination and edge deformation were observed around the drilled holes—phenomena commonly encountered when machining thermoplastic materials—these imperfections were minimal and did not affect the dimensional accuracy or functional performance of the components. The selected 10 mm thickness effectively mitigated such issues while avoiding excess material use, making it a practical and efficient choice for applications involving rapid prototyping, functional testing, and iterative design processes.

The 3D Gence Slicer software was used to adjust key parameters for the MEX process, including shell count, infill percentage, layer thickness, and infill pattern (Fig. 2a). The MEX method facilitates the production of components with hollow structures by employing repetitive internal patterns along the build direction, rather than manufacturing

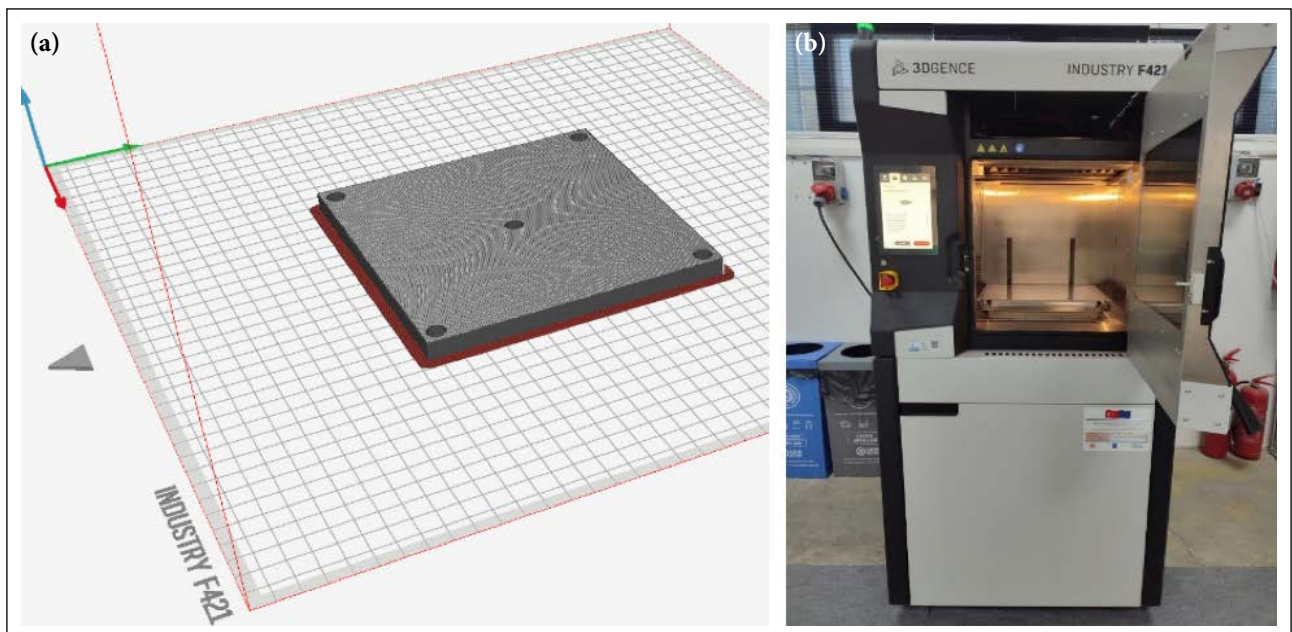


Figure 2. (a) Adapting the design for MEX production using 3D Gence Slicer software (b) 3D GENCE INDUSTRY F421.

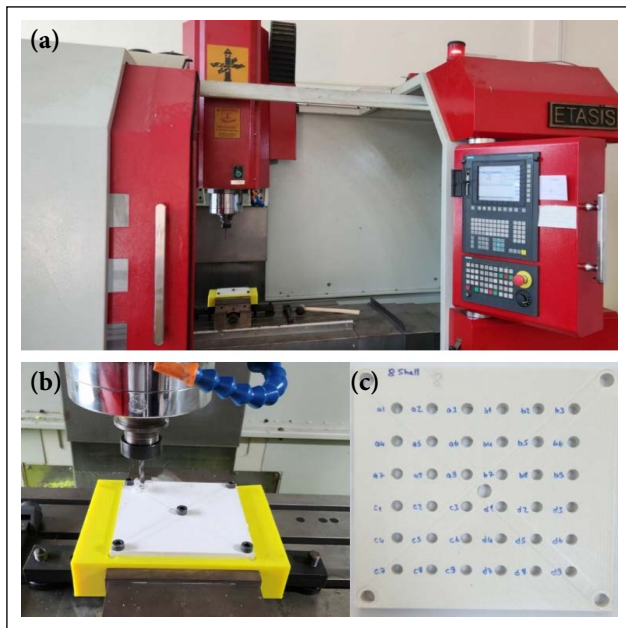


Figure 3. Drilling setup: (a) ETASIS ETAMILL VL1000 VMC, (b) Image captured during the drilling process, (c) Top view of a sample with 8 shell layers after drilling.

fully solid objects. This approach is particularly advantageous for components that are not subjected to significant mechanical stresses, as it reduces weight while maintaining structural integrity. In this study, a zig-zag infill pattern with a 50% infill density was applied to the internal regions of the design.

Layer thickness is a critical parameter that affects mechanical properties, surface finish, and production time. The primary objective of this study was to provide practical insights into post-production drilling operations within typical manufacturing workflows. Therefore, the layer thickness was set to 0.25 mm, a standard value in modern additive manufacturing technologies that offers a balance between quality and production efficiency.

In the MEX method, the hollow regions formed by infill patterns are enclosed by integrated shell layers, which are deposited with a specified overlap. As a result, the external surfaces of the part are fully covered with solid shell layers. In this study, for all samples four shell layers were applied to the bottom surfaces, while the top surfaces—where the drilling tool would penetrate—were manufactured with varying shell layer counts of 4, 8, and 12. The MEX process was conducted using the 3DGence F421 machine (Fig. 2b).

During the manufacturing process, a 1.75 mm diameter PC/ABS (Polymaker™) filament was used as the primary build material, while a 1.75 mm diameter proprietary acrylic copolymer (3D Gence ESM-10) filament was used as the raft material. Prior to manufacturing, both filament materials were dried at 80°C for 16 hours to eliminate any moisture that could affect the printing quality. The primary material was extruded at 280°C, while the raft material was extruded at 250°C. The ambient temperature was maintained at 100°C, and the build plate temperature was set to 105°C. Before printing the main structure, a three-layer raft

Table 1. Process parameters for drilling

Independent variables	Unit	Levels			In total
N: Shell Layer Count	piece	4	8	12	27 combinations
f: Feed Rate	mm/min	50	100	150	
Vc: Spindle Speed	rpm	600	900	1200	

was deposited on the base surface to enhance adhesion and stability. All samples were produced using distinct MEX process parameters.

Surface Roughness Measurement

The surface roughness of the top, bottom and lateral surfaces was measured using a Mitutoyo Surftest SJ-301 profilometer. To evaluate the effect of shell layer count on surface roughness in the lateral region, measurements were conducted exclusively on areas composed of shell layers. The core regions were excluded from analysis, as the process and design parameters in these areas were consistent across all specimens. A Gaussian filter was applied to the measured profiles, with a cut-off length of 0.8 mm and five sampling lengths. The primary surface roughness parameters—Ra (arithmetical mean roughness), Rz (mean peak-to-valley height), and RSm (mean spacing of profile irregularities)—were calculated based on the filtered data.

Drilling Process

The drilling process was performed using an ETASIS ETAMILL VL1000 vertical machining center (VMC) (Fig. 3a). A 6.7 mm diameter high-speed steel (HSS) drill bit was employed for the machining operations. To enable accurate through-hole drilling, a custom fixture was fabricated using the MEX method. This fixture was first mounted on the VMC, and the printed samples were then securely positioned on top of it (Fig. 3b). The selection of a 6.7 mm drill bit was motivated by the need to produce functional prototypes compatible with M8 fasteners—widely used in mechanical design and assembly. In rapid prototyping workflows, parts are frequently manufactured without predefined holes to retain flexibility for post-processing modifications. Standardizing the hole diameter at 6.7 mm, which corresponds to the recommended pilot hole size for M8 threaded connections, allows printed parts to be easily adapted for mechanical fastening without requiring design revisions. This approach facilitates a smoother transition from prototype to functional testing by enabling the direct use of industry-standard fasteners and reducing the need for additional rework during early development stages.

Drilling was performed at three different feed rates and spindle speeds. Each combination of drilling parameters was applied to the samples with three repetitions (Figure 3c). The drilling process was completed in a single pass. After each operation, the tool surfaces were cleaned of chips, and the drill bit was allowed to cool to room temperature before the next drilling cycle.

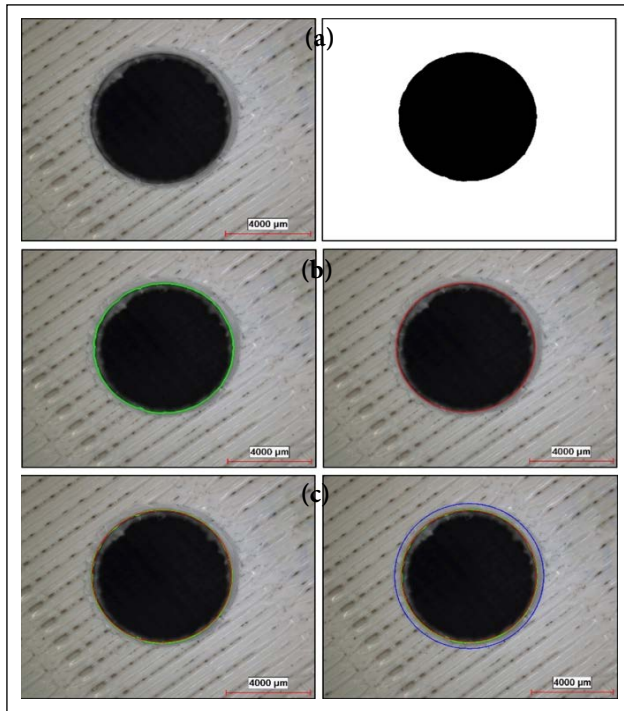


Figure 4. Image processing steps for determining delamination: (a) Image segmentation, (b) Contour detection and circle fitting, (c) Identification of the delamination boundary as a fitted circle.

The independent variables, including the number of shell layers on the top surface, feed rate, and spindle speed, are summarized in Table 1.

Measuring of Diameter and Cylindricity

The entry and exit diameters, along with the cylindricity of the drilled holes, were measured using a Hexagon Coordinate Measuring Machine (CMM), ensuring high precision in assessing dimensional deviations and geometric tolerances. This methodology provided a clear evaluation of how closely the drilled holes conformed to an ideal cylindrical shape. Additionally, detailed imaging was conducted using a stereomicroscope, enabling a thorough examination of hole surfaces, including surface irregularities and burr formation at the exits. The combination of CMM measurements and stereomicroscopic observations allowed for a comprehensive analysis of the drilling process, offering deeper insights into the influence of drilling parameters on machining quality and supporting process optimization.

Image Processing for Determining Delamination

By processing stereomicroscope images, quantitative data can be extracted from circular features. For instance, Ang et al. [25] utilized image processing techniques to analyse cell circularity. In this study, image analysis was employed to detect delamination on the entry and exit surfaces of drilled holes using images captured from these surfaces, leveraging the OpenCV library in Python.

To achieve this, segmentation techniques were applied to mask the images, enabling the separation of the entry and exit profiles of the holes (Fig. 4a). Next, the circular

shape of the hole was reconstructed by merging the point data identified during the analysis. The Hyper Least Squares approach, a circle-fitting technique, was employed to determine the centre and diameter of the hole using the extracted contour data [26]. Figure 4b illustrates the detected contour and the fitted circle, overlaid onto the original image. Using the identified contour and OpenCV functions, the area of the hole was calculated.

These steps were iteratively applied to each image aperture to determine the hole diameters. To enhance visualization, distinctively coloured lines were added to the image to highlight both the hole contour and the fitted circle. The same procedures were applied to the delamination region, where the radially distinct boundaries were isolated. A fitted circle was then generated to match these contours (Fig. 4c), and its diameter and area were calculated. Finally, the area of the hole was subtracted from the delamination contour area to quantify the delamination region.

Statistical Analysis

To comprehensively evaluate the effect of shell layer count on the top and lateral surface quality of the manufactured plates, a one-way analysis of variance (ANOVA) was conducted. Additionally, to assess the influence of machining parameters on hole quality, an n-way ANOVA was performed. This statistical method was employed to systematically analyze the relationships between the independent variables—shell layer count, feed rate, and spindle speed—and the dependent variables, including hole diameter deviation, cylindricity, and delamination. Each parameter was varied within predetermined ranges, allowing the analysis to capture both the main effects of individual factors and any statistically significant interactions among them. For example, the analysis provided insights into whether the effect of feed rate on dimensional accuracy was influenced by variations in spindle speed or shell layer count. The findings from ANOVA offered valuable data for optimizing the machining process, ultimately enhancing both the precision and structural integrity of the final product. The analyses were conducted using Python 3.13 [27] within the Spyder IDE.

RESULTS AND DISCUSSION

Surface Roughness Results

The results for the top surface indicated that the model was not statistically significant for any of the roughness parameters ($p > 0.05$). This outcome is likely due to the presence of both raster infill and shell layers on the top surface, which leads to localized fluctuations in surface texture. As a result, the high variance in the measured data may have masked moderate differences between shell layer conditions. Although the lowest roughness values were observed in the 12-shell condition, it cannot be conclusively stated that shell layer count had a statistically significant effect on top surface roughness (Table 2).

In contrast, shell layer count had a statistically significant effect on the Rz values of the lateral surfaces. However, as shown in Figure 5, no single shell count condition was

Table 2. One-way ANOVA results in surface roughness values on top surfaces

Surface	Independent variable	Dependent variable	Sum of squares	Degree of freedom	Mean square	F-value	p
Top Surface	Shell Count	Ra [μm]	39.26	2	19.63	2.35	0.1760
		Rz [μm]	873.11	2	436.55	2.28	0.1837
			8140.22	2	4070.11	1.3	0.3390
Lateral Surface	Shell Count	Ra [μm]	0.5798	2	0.2899	3.26	0.1098
		Rz [μm]	123.15	2	61.57	69.4	<0.0001
		RSm [μm]	2968.67	2	1484.33	4.5	0.0639

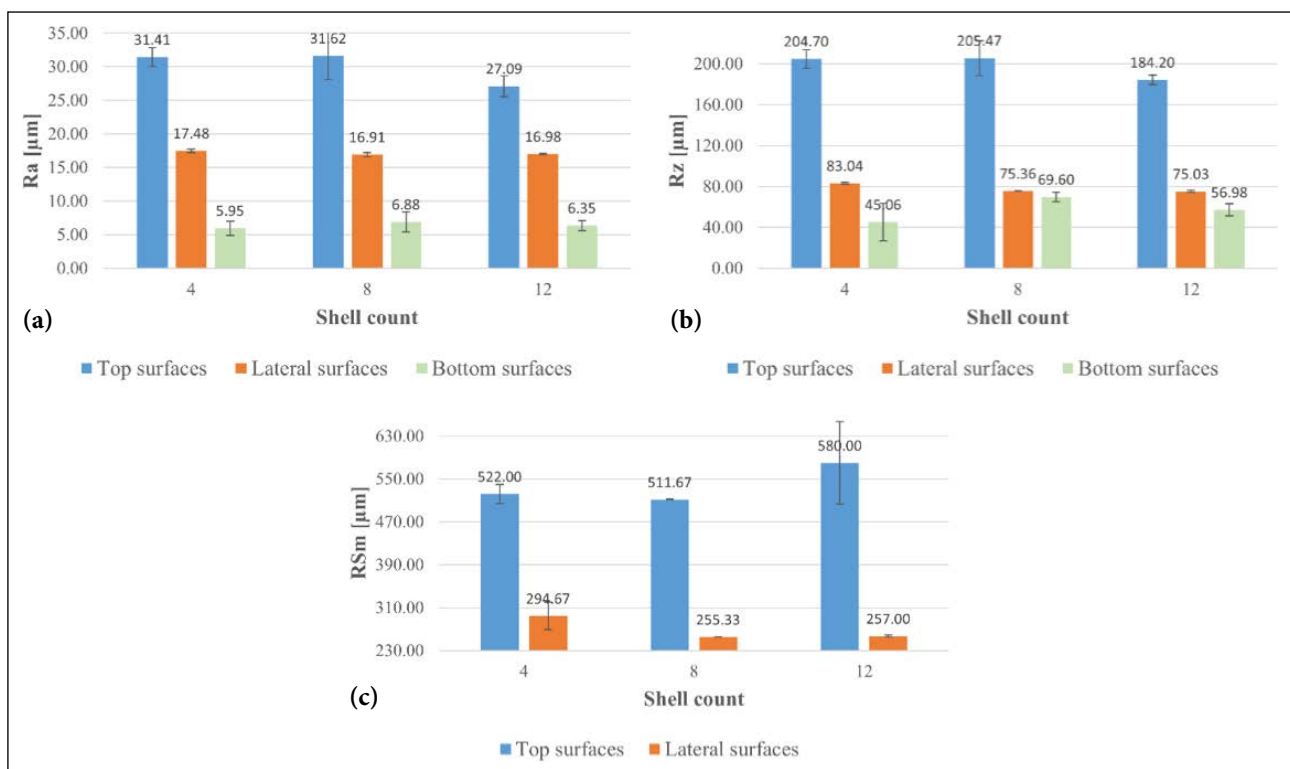


Figure 5. Variations in surface roughness based on shell count on top, lateral and bottom surfaces: (a) Ra, (b) Rz, (c) RSm values.

found to be distinctly superior in terms of surface finish.

The bottom surface, which was printed against a heated raft at 105 °C, is primarily affected by the raft texture and the first-layer squish, rather than by the shell layer count. Minor differences observed in the mean Ra and Rz values are attributed to random variations in first-layer flow and adhesion, rather than to any systematic influence of shell count. Therefore, the relationship between shell layer count and bottom surface roughness was not explored further; the results are reported for reference purposes only.

Additionally, while RSm values were successfully calculated for the top and lateral surfaces, no repeatable surface profile was detected on the bottom surfaces, preventing RSm calculation. This finding supports the explanation that the first-layer squish and the interaction between the build plate and extruded material dominate the bottom surface profile, producing irregularities that do not follow a repeatable pattern.

Deviation in Diameter Results

Table 3 presents the results of the n-way ANOVA analysis for diameter deviation. The analysis revealed that the model was statistically significant ($p < 0.0001$). As observed, the most influential factor affecting diameter deviation was the feed rate, followed by spindle speed as the second most significant parameter. Additionally, the shell layer count was also found to have a statistically significant effect.

Figure 6 illustrates the variation in hole diameter deviation with respect to the examined parameters. The results indicate a clear trend: as the feed rate decreases, the deviation in diameter also decreases. Conversely, higher feed rates lead to an enlargement of the hole diameter. This can be attributed to the fact that increased feed rates generate greater thrust forces, which intensify the tool-workpiece interaction and result in substantial heat buildup during drilling [28]. The elevated temperatures lower the viscosity of the thermoplastic material, causing localized deforma-

Table 3. N-way ANOVA results in deviation in diameter values

	Sum of squares	Degree of freedom	Mean square	F-value	p
Model	0.0611	6	0.0102	11.91	<0.0001
Shell count	0.0103	2	0.0051	6.02	0.0034
Feed rate	0.0275	2	0.0137	16.07	<0.0001
Spindle speed	0.0234	2	0.0117	13.65	<0.0001

tion around the hole and ultimately leading to permanent expansion of the hole diameter [29]. Supporting this observation, Srinivasan et al. [17] reported that, in the drilling

of glass fiber-reinforced polycarbonate, increasing the feed rate led to a rise in thrust force of up to 45%, establishing a clear correlation between feed rate, cutting forces, and dimensional enlargement.

Another possible contributor to hole diameter expansion is vibration, or chatter, which is associated with the dynamic behavior of the drill bit during operation [30]. As feed rate increases, the cutting forces become more intense, raising the potential for chatter. These vibrations can cause rapid fluctuations in cutting forces, resulting in irregular tool engagement and inconsistent material removal. Additionally, chatter may lead to the formation of rough surface textures around the hole, making it more difficult to achieve precise diameter measurements and reducing dimensional accuracy.

In contrast, an increase in spindle speed was found to reduce diameter deviation. This is likely due to improved

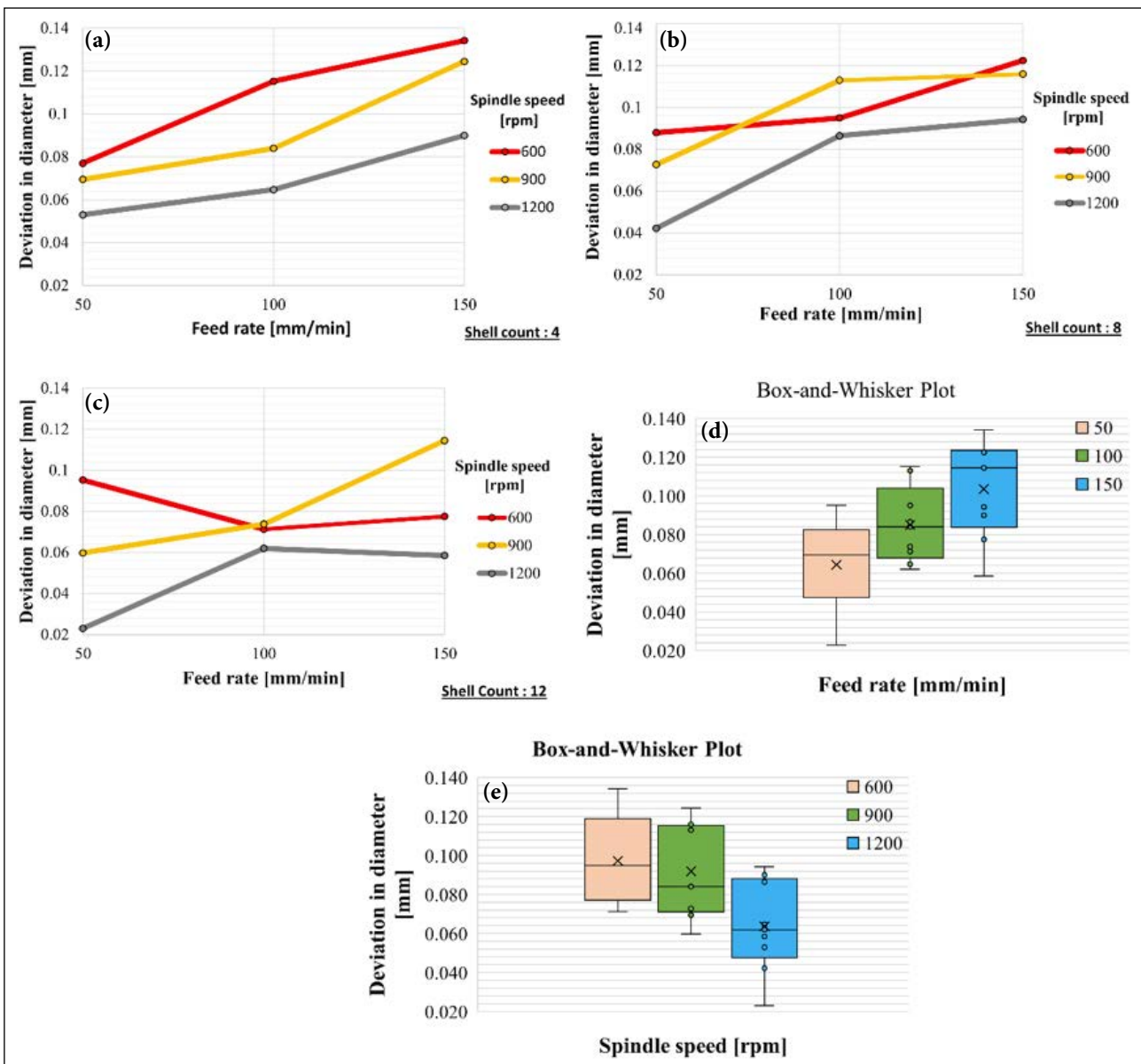


Figure 6. Variations in diameter deviation based on feed rate and spindle speed parameters: (a) Shell count = 4, (b) Shell count = 8, (c) Shell count = 12. (d) Average deviation for different feed rate values. (e) Average deviation for different spindle speed values.

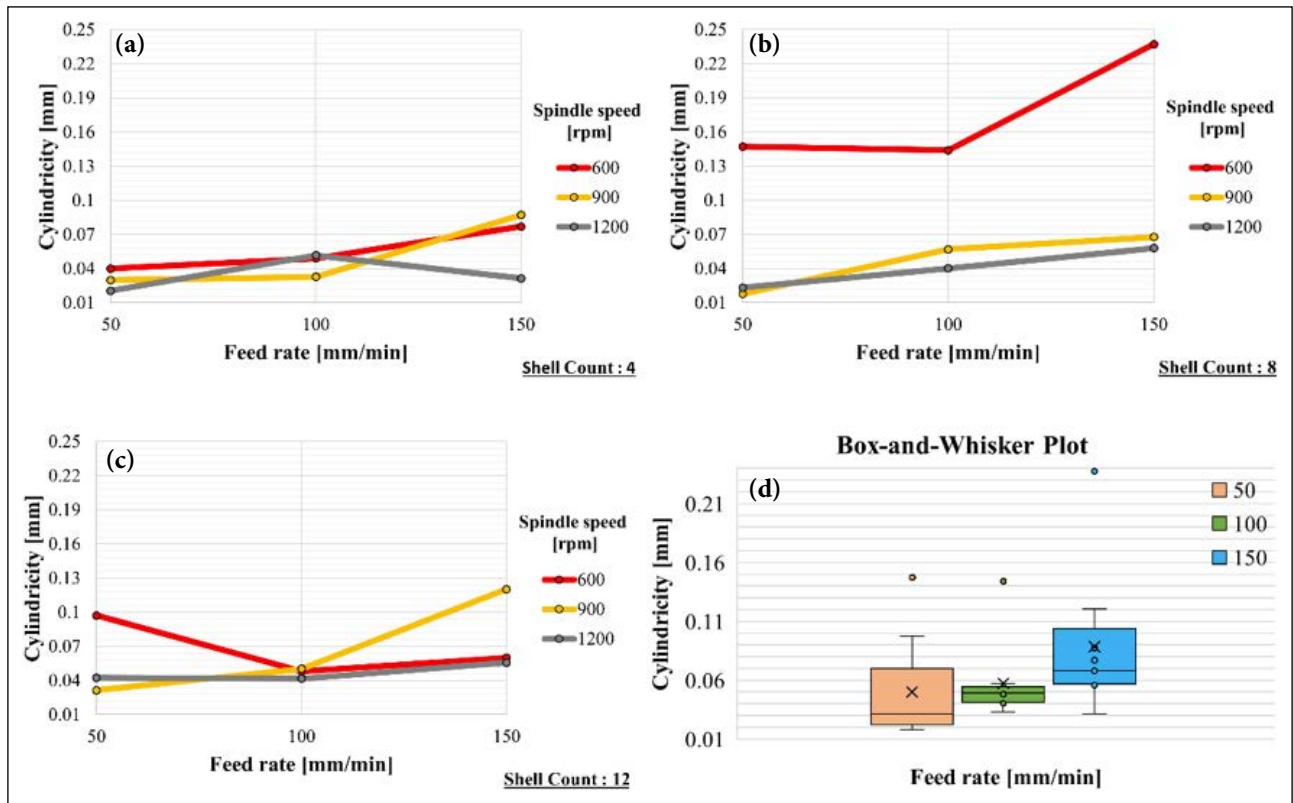


Figure 7. Variations in cylindricity based on feed rate and spindle speed parameters: (a) Shell count = 4, (b) Shell count = 8, (c) Shell count = 12. (d) Average cylindricity for different feed rate values.

thermal softening and chip evacuation at higher speeds, which facilitate smoother cutting and minimize thermal-induced expansion. Therefore, combining a low feed rate with a high spindle speed is recommended for achieving higher precision in drilled holes.

No significant trend was observed between shell layer count and hole diameter deviation, as shown in Figure 5a–c. Furthermore, Figure 5d–e presents Box-and-Whisker plots illustrating the effects of the independent variables—excluding shell layer count—on diameter deviation. These plots confirm that the lowest deviations occurred under conditions of low feed rate and high spindle speed. An additional noteworthy observation is that, throughout the drilling of PC/ABS samples, only diameter expansion was observed; no evidence of hole shrinkage was detected.

Cylindricity Results

The n-way ANOVA analysis conducted for cylindricity values revealed that the model was statistically significant ($p=0.0209$). As presented in Table 4, among the evaluated parameters, feed rate was the only factor found to have a statistically significant effect on cylindricity.

Figure 7 illustrates the variation in cylindricity values with respect to different machining parameters. The results indicate that cylindricity worsens as the feed rate increases. In contrast, no consistent trend was observed between spindle speed, shell layer count, and cylindricity (Figure 7a–c). Additionally, Figure 7d presents a Box-and-Whisker plot showing the influence of the independent variables—excluding shell layer count—on cylindricity. Given that the

Table 4. N-way ANOVA results in cylindricity values

	Sum of squares	Degree of freedom	Mean square	F-value	p
Model	0.1309	6	0.0218	2.63	0.0209
Shell count	0.0319	2	0.0160	1.92	0.1519
Feed rate	0.0298	2	0.0149	1.80	0.1712
Spindle speed	0.0691	2	0.0346	4.16	0.0184

ideal cylindricity value is zero, the plot clearly demonstrates that higher feed rates lead to increased deviation from ideal cylindricity. These findings underscore the importance of selecting an optimal combination of spindle speed and feed rate to minimize cylindricity errors and improve hole quality in MEX-manufactured PC/ABS parts.

Higher cutting forces due to an increasing feed rate can cause deviations from linear motion, leading to cylindricity errors. Additionally, increasing the feed rate enhances the interaction and vibrations between the drill and the workpiece. These vibrations can cause fluctuations in hole diameter, which may result in increased cylindricity errors. Previous studies support these findings, as demonstrated by Ameer et al. [31], which highlight the impact of increased feed rate on cylindricity errors in composite materials. Similarly, Maoinsier et al. [32] also emphasize that higher feed rates generate more thrust force, which can further exacerbate cylindricity errors.

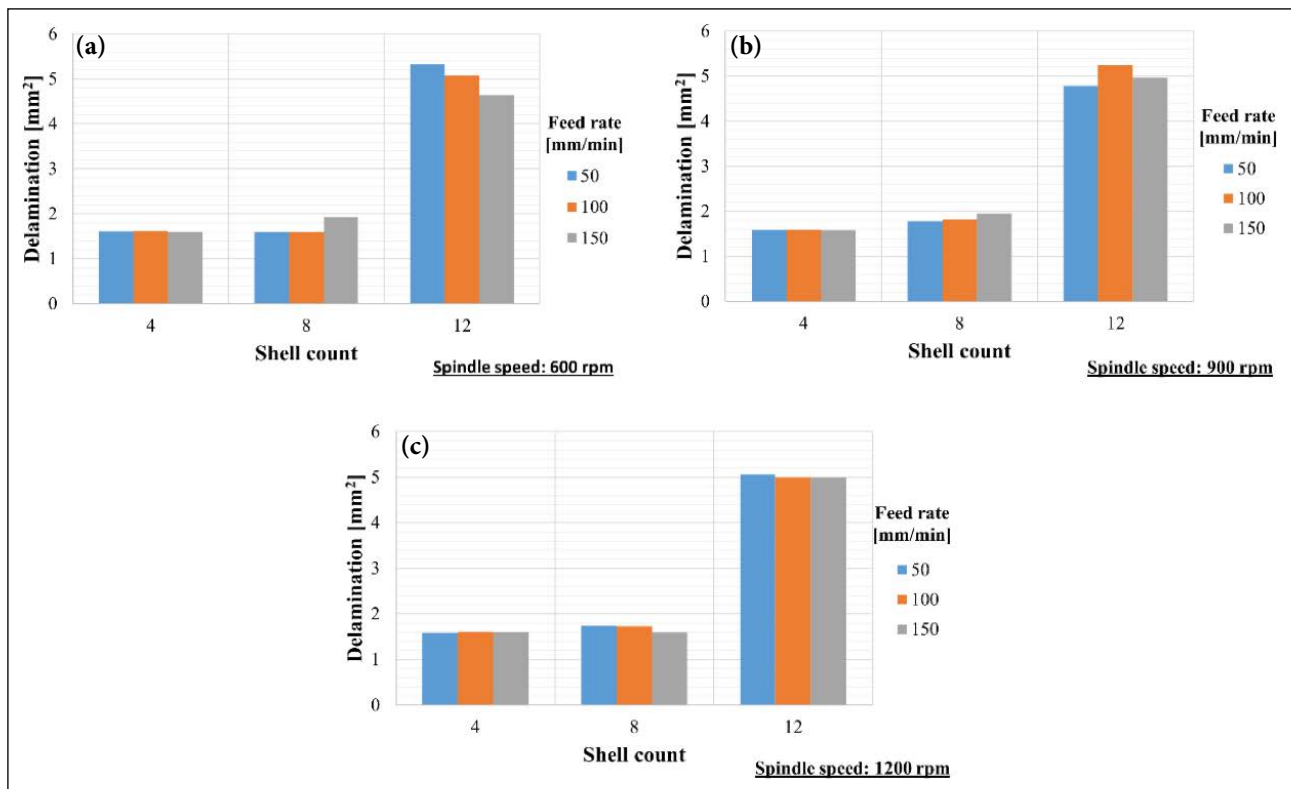


Figure 8. Variations in delamination based on shell count and feed rate parameters: (a) Spindle speed = 600 rpm, (b) Spindle speed = 900 rpm, (c) Spindle speed = 1200 rpm.

Delamination Results

The n-way ANOVA analysis for delamination revealed that the model was statistically significant ($p < 0.0001$). As shown in Table 5, shell layer count had a highly significant effect on delamination ($p < 0.0001$). In contrast, the p-values associated with feed rate and spindle speed indicate that these parameters did not have a statistically significant influence on delamination levels.

Figure 8 illustrates the variation in delamination levels with respect to shell layer count, spindle speed, and feed rate. The results indicate that delamination remained low and comparable at shell counts of 4 and 8, but increased significantly at a shell count of 12. Therefore, for components intended to undergo post-production drilling, maintaining a shell layer count between 4 and 8 is recommended to minimize delamination (Fig. 8). In contrast, no consistent trend was observed between delamination and either feed rate or spindle speed.

As the number of shell layers increases, the outer walls of the printed part may become thicker and denser, potentially requiring a greater thrust force during drilling [33]. This elevated thrust force could lead to stress concentration, particularly near the exit surface of the hole. The accumulated stress might cause upward displacement of the underlying layers. If the interlayer adhesion is insufficient to resist this stress, the layers may separate, possibly resulting in delamination. Consequently, an increase in shell count might raise both the thrust force and the risk of delamination during the drilling process.

Table 5. N-way ANOVA results in delamination values

	Sum of Squares	Degree of Freedom	Mean Square	F-value	p
Model	262.07	6	43.68	177.47	<0.0001
Shell Count	261.85	2	130.92	531.97	<0.0001
Feed Rate	0.0360	2	0.0180	0.0731	0.9296
Spindle Speed	0.0398	2	0.0199	0.0809	0.9224

CONCLUSION

In this study, the effect of shell layer count in the Material Extrusion (MEX) process on the surface roughness and the drilling performance of additively manufactured parts was investigated. Specifically, the research focused on how drilling, as a secondary operation, impacts hole quality in MEX-fabricated components. Drilling experiments were performed at various spindle speeds and feed rates to identify optimal process parameters. Deviations in hole diameter, cylindricity, and surface delamination were measured, and their relationships with the independent variables were analyzed using both one-way and n-way ANOVA. The findings provide quantitative evidence of trends that can guide designers and engineers in making informed decisions. Notably, the results reveal that variations in shell layer count can subtly influence outcomes such as delamination and surface finish—offering new insights into post-processing strategies for additively manufactured components.

The following conclusions were drawn from the study:

- Shell layer count did not have a statistically significant effect on top surface roughness, likely due to the influence of raster infill and localized variability. Its effect on the lateral surface was also limited; however, a statistically significant impact was observed for Rz on the lateral surfaces. While surface quality showed slight improvement at higher shell counts, no single condition proved to be distinctly superior.
- The deviation in hole diameter exhibited a positive correlation with feed rate and a negative correlation with spindle speed, while no significant relationship was observed with shell layer count. The primary cause of oversized holes relative to the nominal diameter is the variation in cutting temperature, which is influenced by feed rate and cutting speed.
- The cylindricity value increased with higher feed rates, whereas spindle speed and shell layer count had no statistically significant effect.
- Delamination remained low and comparable for shell counts of 4 and 8 but increased significantly at a shell count of 12.
- No specific trend or correlation was identified between delamination and the variables of feed rate or spindle speed.
- Based on these findings, it is recommended that designs requiring drilled holes be manufactured with 4 or 8 shell layers, followed by drilling at a feed rate of 50 mm/min and a spindle speed of 1200 rpm. These results are expected to provide valuable insights for industrial applications.

Data Availability Statement

The authors confirm that the data that supports the findings of this study are available within the article. Raw data that support the finding of this study are available from the corresponding author, upon reasonable request.

Author's Contributions

Firat Mavi: Conception, Design, Materials, Data Collection and Processing, Analysis and Interpretation, Literature Reviewer, Writer.

Kemal Ayan: Conception, Data Collection and Processing, Analysis and Interpretation, Writer, Literature Review.

Nail Aslan: Conception, Data Collection and Processing, Writer, Literature Review.

Sırrı Can Polat: Conception, Data Collection and Processing.

İbrahim Etem Saklakoğlu: Conception, Design, Materials, Supervision, Data Collection and Processing, Critical Review.

Nurşen Saklakoğlu: Conception, Design, Materials, Supervision, Data Collection and Processing, Writer, Literature Reviewer, Critical Review.

Conflict of Interest

The authors declared no potential conflicts of interest with respect to the research, authorship, and/or publication of this article.

Use of AI for Writing Assistance

Not declared.

Ethics

There are no ethical issues with the publication of this manuscript.

REFERENCES

- [1] ISO/ASTM International (2022). ISO/ASTM 52900-21: Additive manufacturing - General principles - Fundamentals and vocabulary. ISO/ASTM International.
- [2] ISO/ASTM International (2020). ISO/ASTM 52903-1:2020(E): *Additive manufacturing - Material extrusion-based additive manufacturing of plastic materials - Part 1: Feedstock materials*. ISO/ASTM International.
- [3] Simon, Ž., Stojcevski, F., Dharmasiri, B., Amini, N., Stojcevski, F., & Henderson, C. L. (2024). Circular economy-driven additive manufacturing: A model for recycling PLA/copper composites through multi-extrusion processing. *Journal of Industrial and Engineering Chemistry*, 130, 392-400. [CrossRef]
- [4] Altıparmak SC, Daminabo SIC (2024). Suitability analysis for extrusion-based additive manufacturing process. *Additive Manufacturing Frontiers*, 3, Article 200106. [CrossRef]
- [5] Kartal, F., & Kaptan, A. (2023). Experimental determination of the optimum cutting tool for CNC milling of 3D printed PLA parts. *International Journal of 3D Printing Technologies and Digital Industry*, 7, 150-160. [CrossRef]
- [6] Golubovic, Z., Bojovic, B., Petrov, L., Milovanovic, A., Milosevic, M., Bojovic, B., Sedmak, A., & Miskovic, Z. (2024). Comparative analysis of ABS materials mechanical properties. In: *Procedia Structural Integrity* (pp. 153-159). Elsevier B.V. [CrossRef]
- [7] Pour, R. H., Hassan, A., Soheilmoghaddam, M., & Bidsorkhi, H. C. (2016). Mechanical, thermal, and morphological properties of graphene-reinforced polycarbonate/acrylonitrile butadiene styrene nanocomposites. *Polymer Composites*, 37, 1633-1640. [CrossRef]
- [8] Kuczynski, J., Snyder, R. W., & Podolak, P. P. (1994). Physical property retention of PC/ABS blends. *Polymer Degradation and Stability*, 43, 285-291. [CrossRef]
- [9] Zhang, W., & Xu, Y. (2019). *Mechanical properties of polycarbonate: Experiment and modeling for aeronautical and aerospace applications*. 1st ed. Elsevier.
- [10] Utracki, L. A. (2002). *Polymer blends handbook*. Kluwer Academic Publishers. [CrossRef]
- [11] Choi, H. J., Park, S. H., Kim, K., & Jun, J. I. (2000). Effects of acrylonitrile content on PC/ABS alloy systems with a flame retardant. *Journal of Applied Polymer Science*, 75, 417-423. [CrossRef]
- [12] Balakrishnan, S., & Neelakantan, N. R. (1998). Mechanical properties of blends of polycarbonate with unmodified and maleic anhydride grafted ABS. *Polymer International*, 45, 347-352. [CrossRef]

- [13] Fang, Q. Z., Wang, T. J., & Li, H. M. (2006). Large tensile deformation behavior of PC/ABS alloy. *Polymer (Guildford)*, 47, 5174-5181. [CrossRef]
- [14] Seelig, T., & Van der Giessen, E. (2002). Localized plastic deformation in ternary polymer blends. *International Journal of Solids and Structures*, 39, 3505-3522. [CrossRef]
- [15] Raj, M. M. (2014). Studies on mechanical properties of PC-ABS blends. *Journal of Applied Sciences and Engineering Research*, 3(2), 512-518.
- [16] Alonso, U., Goirigolzarri, B., Ostra, T., & De Lacalle, L. N. L. (2019). Low frequency vibration assisted drilling of PC1000 polycarbonate. *Procedia Manufacturing*, 41, 407-414. [CrossRef]
- [17] Srinivasan, T., Palanikumar, K., & Rajagopal, K. (2014). Influence of thrust force in drilling of glass fiber reinforced polycarbonate (GFR/PC) thermoplastic matrix composites using Box-Behnken design. *Procedia Materials Science*, 5, 2152-2158. [CrossRef]
- [18] Abdulwahab, A. E., Hubeatir, K. A., & Imhan, K. I. (2022). A comparative study on the effect of CO₂ laser parameters on drilling process of polycarbonate and PMMA polymers complemented by design expert. *Engineering Research Express*, 4(4), Article 045029. [CrossRef]
- [19] Szot, W., & Rudnik, M. (2024). Effect of the number of shells on selected mechanical properties of parts manufactured by FDM/FFF technology. *Advances in Materials Science*, 24(1), 86-103. [CrossRef]
- [20] Qamar Tanveer M, Mishra G, Mishra S, Sharma R (2022). Effect of infill pattern and infill density on mechanical behaviour of FDM 3D printed parts - a current review. *Materials Today: Proceedings*, 62, 100-108. [CrossRef]
- [21] Yazdani Sarvestani, H., Akbarzadeh, A. H., Mirbolghasemi, A., & Hermenean, K. (2018). 3D printed meta-sandwich structures: Failure mechanism, energy absorption and multi-hit capability. *Materials & Design*, 160, 179-193. [CrossRef]
- [22] Charekhli-Inanillo, M., & Mohammadimehr, M. (2023). The effect of various shape core materials by FDM on low velocity impact behavior of a sandwich composite plate. *Engineering Structures*, 294, Article 116721. [CrossRef]
- [23] Mirzaei, J., Niyaraki, M. N., & Nikouei, S. M. (2025). Mechanical characteristics of 3D-printed honeycomb sandwich structures: Effect of skin material and core orientation. *Polymer Composites*. Preprint. <https://doi.org/10.1002/pc.29610> [CrossRef]
- [24] Khoran, M., Ghabezi, P., Frahani, M., & Besharati, M. K. (2015). Investigation of drilling composite sandwich structures. *International Journal of Advanced Manufacturing Technology*, 76, 1927-1936. [CrossRef]
- [25] Ang, M., Konstantopoulo, A., Goh, G., Htoon, H. M., Seah, X., Lwin, N. C., Liu, X., Chen, S., Liu, L., & Mehta, J. S. (2016). Evaluation of a micro-optical coherence tomography for the corneal endothelium in an animal model. *Scientific Reports*, 6, Article 29769. [CrossRef]
- [26] Kanatani, K., & Rangarajan, P. (2011). Hyper least squares fitting of circles and ellipses. *Computational Statistics & Data Analysis*, 55, 2197-2208. [CrossRef]
- [27] Van Rossum, G., & Drake, F. (2009). *Python 3 Reference Manual*. CreateSpace, Scotts Valley, CA.
- [28] Lotfi, A., Li, H., & Dao, D. V. (2019). Machinability analysis in drilling flax fiber-reinforced polylactic acid bio-composite laminates. *Int Scholar Scientif Res Innov*, 13(9), 443-447.
- [29] Krishnamoorthy, A., Boopathy, S. R., & Palanikumar, K. (2009). Delamination analysis in drilling of CFRP composites using response surface methodology. *Journal of Composite Materials*, 43, 2885-2902. [CrossRef]
- [30] Endo, H., & Marui, E. (2006). Small-hole drilling in engineering plastics sheet and its accuracy estimation. *International Journal of Machine Tools and Manufacture*, 46, 575-579. [CrossRef]
- [31] Ameur, M. F., Habak, M., Kenane, M., Aouici, H., & Cheikh, M. (2017). Machinability analysis of dry drilling of carbon/epoxy composites: Cases of exit delamination and cylindricity error. *International Journal of Advanced Manufacturing Technology*, 88, 2557-2571. [CrossRef]
- [32] Maoinsar, M. A., Ahmad, F., & Sharif, S. (2014). Effects of cutting parameters on hole integrity when drilling GFRP and HFRP composites. *Advanced Materials Research*, 845, 960-965. [CrossRef]
- [33] Pachappareddy, C., Padhy, C. P., & Pendyala, S. (2025). An experimental investigation on delamination factor and thrust force evaluation of kenaf fiber and acacia concinna filler reinforced epoxy hybrid composites. *Green Technologies and Sustainability*, 3, Article 100164. [CrossRef]